

First-principles study of the electronic structure of γ -InSe and β -InSe

P. Gomes da Costa

*University of Rochester, Rochester, New York 14627
and Xerox Webster Research Center, Webster, New York 14580*

R. G. Dandrea

Xerox Webster Research Center, Webster, New York 14580

R. F. Wallis

Department of Physics, University of California, Irvine, California 92717

M. Balkanski

Laboratoire de Physique des Solides, Université Pierre et Marie Curie, 4 place Jussieu, 75252 Paris CEDEX 05, France

(Received 18 June 1993)

The electronic band structure of the semiconducting β and γ polytypes of InSe is calculated from first principles, with spin-orbit effects included. The two polytypes differ by the lateral stacking arrangement of four-atomic-plane building blocks, composed of Se-In-In-Se planes. These building blocks are terminated by Se lone-pair orbitals, which form the electronic states at the valence-band maximum. There is very little bonding between these four-atomic-plane units, and so the band structures of the γ and β polytypes are nearly identical, being related simply by zone folding. We find that both materials have direct band gaps (which occur at the Γ and Z points in the Brillouin zone for the β and γ polytypes, respectively), and that there is a large dipole matrix element (i.e., a strong oscillator strength) between the valence maximum and conduction minimum states. These materials are thus potentially significant for light emitting and absorbing devices. In order to study the optical absorption at energies above the band gap, the imaginary part of the dielectric function $\epsilon_2(\omega)$ is calculated for $\omega \leq 12$ eV. The effective masses are also calculated: the out-of-plane masses are extremely light, and are equal in magnitude at the valence maximum and conduction minimum states ($m_{\perp}^v = m_{\perp}^c \approx 0.03m_0$), while the in-plane masses are light for the electrons ($m_{\parallel}^e \approx 0.1m_0$) and heavy for the holes ($m_{\parallel}^h \approx 3m_0$). The "anomalous" mass character ($m_{\perp} < m_{\parallel}$) is explained in terms of intralayer bonding and the lack of lateral bonding between the Se lone-pair orbitals that constitute the valence maximum states.

I. INTRODUCTION

InSe is a layered compound having complex layers in which atomic layers of Se, In, In, and Se are bound together by covalent bonds with some ionic character. Each atomic plane is a (111) plane in a conventional zinc-blende structure. These complex layers are themselves bound to one another by weak Van der Waals interactions with a so-called Van der Waals gap between layers. There are four possible stacking arrangements of the complex layers leading to four polytypes designated β , ϵ , γ , and δ . Only three of these polytypes (β , ϵ , γ) have been observed for InSe. They correspond to the three ways of stacking successive layers: the first corresponds to a rotation by π around an axis perpendicular to the plane of the layer followed by a translation parallel to the axis of rotation (the β polytype); the other two ways correspond to a translation where the horizontal components are $-(\mathbf{a}_1 + \mathbf{a}_2)/3$ in one case (ϵ polytype) and $(\mathbf{a}_1 + \mathbf{a}_2)/3$ in the other (γ polytype), where the \mathbf{a} 's are the basis vectors of a hexagonal lattice. We have studied two of those polytypes: the β polytype which has a hexagonal crystal lattice with two complex layers (eight atoms) per unit cell and the γ polytype with a rhombic or

trigonal crystal lattice containing only one complex layer (four atoms) in the unit cell. Figure 1 shows the stacking of three of those layers in the case of the γ polytype of InSe. Beyond its intrinsic attraction as a two-dimensional material, InSe is known to have promising technical applications, e.g., it is a very good candidate for the cathode material in solid-state batteries.^{1,2} Not surprisingly, in the last 20 years, many investigations have been done on InSe as well as the similar semiconducting III-VI layer compounds GaS and GaSe.¹ The first band structure for this family of materials was calculated for GaSe,³ using an empirical pseudopotential method. A calculation for β -InSe within a tight-binding model has been carried out in a two-dimensional approximation.⁴ Extensions to the three-dimensional case have been developed using an empirical pseudopotential method⁵ and a tight-binding method.^{6,7} Including the spin-orbit interaction in the tight-binding calculation⁸ has a non-negligible effect on the InSe band structure. Empirical pseudopotential calculations for ϵ -InSe are also available,⁹ but without spin-orbit interaction. Although many of the experimental results that have been obtained are for γ -InSe, all of these calculations mentioned previously were done for the β and ϵ polytypes. We calculat-

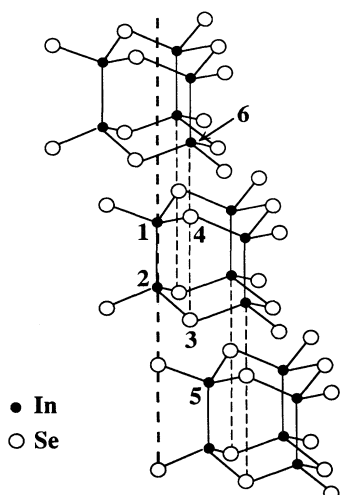


FIG. 1. Perspective view of three layers of γ -InSe. The primitive unit cell extends over one layer and is rhombohedral (2 In and 2 Se atoms). Alternatively, a hexagonal unit cell extending over three layers can be considered. Within a layer one recognizes the pyramidal p^3 coordination of Se atoms and the tetrahedral sp^3 coordination of In atoms. The fundamental crystal parameters are $a = 4 \text{ \AA}$, $c = 24.95 \text{ \AA}$ (includes three layers as in the figure), $d_{\text{In-In}} = 2.80 \text{ \AA}$, and $d_{\text{In-Se}} = 2.64 \text{ \AA}$.

ed, in a previous paper,¹ the band structure of γ -InSe using a tight-binding method. However, a first-principles calculation involving γ -InSe was not done until 1988 by Kunc and Zeyher.¹⁰ They studied the diffusion path of Li in γ -InSe by means of total-energy calculations; no electronic band structure was presented. Here they focused on the γ polytype, because this is the one currently grown by the Bridgeman method.¹ In the past there has been some confusion as to whether the experimentally grown InSe was of the β or γ polytype. The difference in total energy between the various polytypes is so small that one practically always finds a high density of stacking faults in a given sample. To compare with previous calculations, we studied both γ - and β -InSe. The *ab initio* method we used is based on the density-functional theory (DFT);¹¹ the plane-wave pseudopotential method^{12,13} and the local-density approximation (LDA) (Ref. 14) to DFT were used here. A development of the local-density functional theory used in the present work is described in Sec. II. The electronic band structure of both β - and γ -InSe are presented in Sec. III. We find that these materials are direct-gap semiconductors with very light masses of both electrons and holes normal to the layers, their out-of-plane effective mass being $m_1^* \approx 0.03$ in units of free-electron mass. These results are compared with a previous calculation we have done¹ using a tight-binding method based on a procedure by Doni *et al.*⁷ called the overlap-reduced semiempirical tight-binding method. Section IV describes some optical properties we calculated: the density of states (DOS), the joint density of states [$J_{cv}(\epsilon)$], and the imaginary part of the dielectric function $\epsilon_2(\omega)$. Concluding remarks are made in Sec. V.

II. COMPUTATIONAL METHOD

Our calculations were performed using local-density functional theory¹¹ and the *ab initio* pseudopotential method. We employed the nonlocal norm-conserving ionic pseudopotentials of Kerker,¹³ for In and Se.

The wave functions were expanded in plane waves with kinetic energy up to 20 Ry. To test convergence with respect to the basis set size we calculated the gap at three different points in the Brillouin zone (at Γ , B , and Z for γ -InSe and at Γ , M , and A for β -InSe; see Sec. III) at different cutoff energies. The values of these gaps at a 25-Ry cutoff differ from those at the 20-Ry cutoff by less than 10^{-2} eV and are considered accurate enough for our band-structure calculations. The method of special k points¹⁵ was used to perform the integrations in k space over the first Brillouin zone; ten and four k points in the reduced Brillouin zone were used for γ - and β -InSe, respectively. Broyden's technique¹⁶ was used to achieve self-consistency. The self-consistent iterations were continued until the maximum difference between the input and output potentials reached 10^{-4} Ry. In a first-principles LDA calculation, the exchange-correlation energy is not an adjustable function; it is locally defined to be the exchange-correlation energy of a homogeneous electron gas. The function which is now widely accepted as the most accurate is the energy calculated numerically for a large range of densities by Ceperley and Alder¹⁴ using Monte Carlo techniques. An analytic fit to these results by Perdew and Zunger¹⁷ is used in our calculations. Once self-consistency is attained we calculate the total energy using the expressions given in Ihm, Zunger, and Cohen.¹²

Scalar relativistic effects were included in the pseudopotentials, and spin-orbit effects were included perturbatively (using the self-consistent potential and charge density from the scalar calculation) in a first-principles manner.¹⁸ The spin-orbit effects on the band structure of InSe are shown to be non-negligible.

III. THE ELECTRONIC STRUCTURE

The electronic band structure of γ -InSe (neglecting spin-orbit effects) is shown in Fig. 2 for the high-symmetry directions in the first Brillouin zone (BZ). The

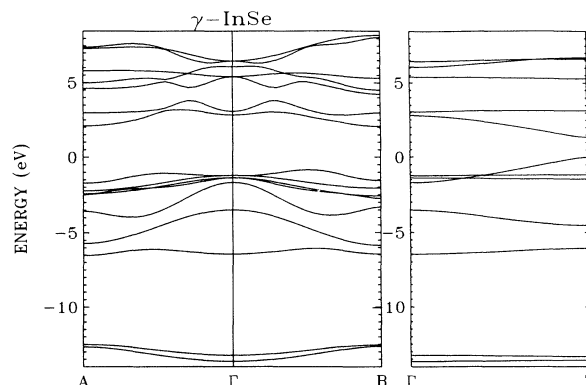


FIG. 2. Electronic band structure of γ -InSe.

notation for the high-symmetry points is that of Slater¹⁹ for the trigonal system with space group C_{3v}^5 . The fundamental gap is direct and occurs at Z , i.e., at the BZ edge going in a direction perpendicular to the layers. Its calculated value is 0.34 eV; as is well known, LDA calculations consistently underestimate the value of the gaps; the “scissors operator” was used to shift rigidly the conduction bands so that the fundamental gap is set equal to 1.35 eV, an experimentally determined value.²⁰ Figure 3 shows the electronic band structure of β -InSe (without spin-orbit effects) for several high-symmetry directions in the first Brillouin zone. The crystal lattice for this polytype is hexagonal with space group D_{6h}^4 , and we followed the same notation as in our previous paper¹ for the high-symmetry points in the reciprocal space. Use was once again made of the “scissors operator” to rigidly shift the conduction bands in order to have the fundamental gap set to 1.35 eV. The difference between the γ and β polytypes is due to a different relative orientation between stacking layers in the two polytypes. Since the interaction between layers is weak (due to Van der Waals forces), we expect the two polytypes to have a very similar electronic structure, in agreement with the previous work of le Toullec *et al.*²¹ This is shown in Fig. 4: β -InSe, having two four-atomic-plane layers per unit cell, has nearly identical energy bands as γ -InSe, having one four-atomic-phase layer per unit cell and hence a nearly twice as big BZ (it would be exactly twice if the stackings of layers were exactly the same in both cases). Folding the bands halfway along ΓZ (in the direction of layer stacking) for γ -InSe gives very nearly the band structure for β -InSe, the small differences being due to the weak interlayer coupling. The effects of including the spin-orbit interactions in our band structure of γ -InSe are shown in Fig. 5. Comparison with the non-spin-orbit band structure of Fig. 4 shows that the nondegenerate (discounting spin) valence maximum and conduction minimum states at Z are not affected by the spin-orbit interaction, while the doubly degenerate second and third valence bands at Z are each split by about 0.3 eV. There are also the two top valence bands that are split at Γ .

The present results for γ -InSe are in disagreement with our previous tight-binding calculations,¹ where the minimum gap was also direct, but at the center of the BZ at Γ . The discrepancy arises from using in the calcula-

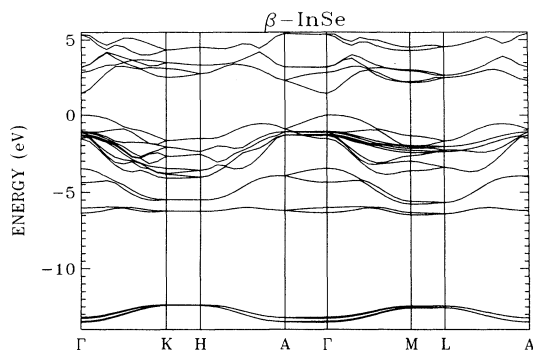


FIG. 3. Electronic band structure of β -InSe.

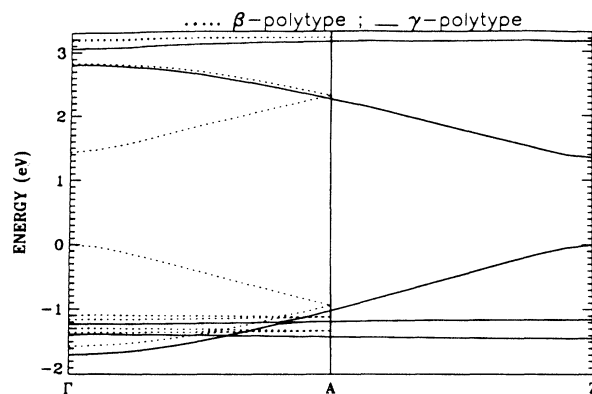


FIG. 4. Folding of the bands along k_z in going from the γ to the β polytype.

tion of the tight-binding parameters for γ -InSe a set of parameters taken from a calculation for β -InSe and then adjusting them in a way such that the minimum of the gap at Γ agrees with experimental optical-absorption data;²⁰ this shows the error inherent in tight-binding calculations when parameters for the atomic orbital overlaps are transferred from one polytype to another. Comparing the β -InSe band structure with previous work,^{1,7} it can be noted that there is a relatively good agreement between the calculations, except for the nature of the gap; the present calculation gives a direct gap at Γ , whereas previously¹ we had an indirect gap between Γ and M that was somewhat smaller than the direct gap at Γ .

Figure 6 shows the total valence charge density for γ -InSe. It can be observed that there is no bonding between layers. The charge densities for the bottom conduction and top valence bands are shown in Fig. 7 for a plane containing the sequence Se-In-In-Se of atoms and extending from one layer to half of the second layer immediately above. Atoms and intralayer bonding directions are indicated. The asymmetry between the top and bottom Se atoms in a layer is due to the atomic structure (see Fig. 1; the interlayer environment for atom 4 is

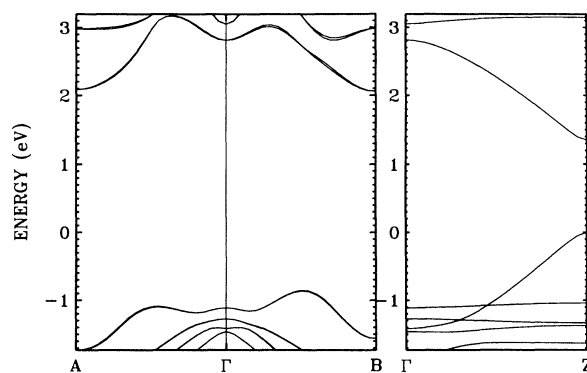


FIG. 5. Band structure of γ -InSe with spin-orbit effects included.

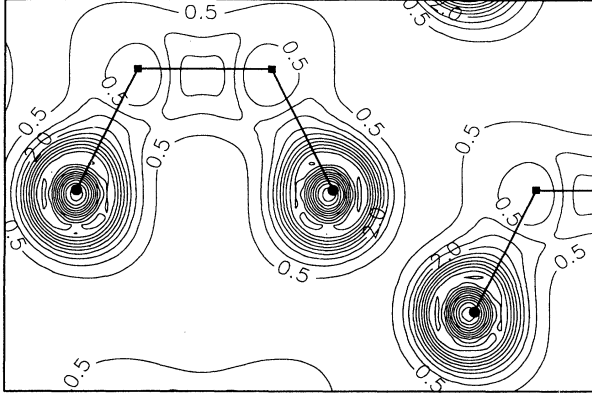


FIG. 6. Calculated valence charge density of γ -InSe with spin-orbit effects included. The straight lines joining pairs of atoms are a guide for the eye. The atom positions are represented by filled circles in the case of Se and filled squares in the case of In. The numbers indicate the relative charge density.

different from the one for atom 3). Figure 7(b) for the valence-band maximum shows a nonbonding lone-pair p_z orbital on Se and a σ bonding orbital between In-In. Figure 7(a) for the conduction-band minimum shows antibonding orbitals for In and Se atoms.

The effective electron and hole masses for γ -InSe were

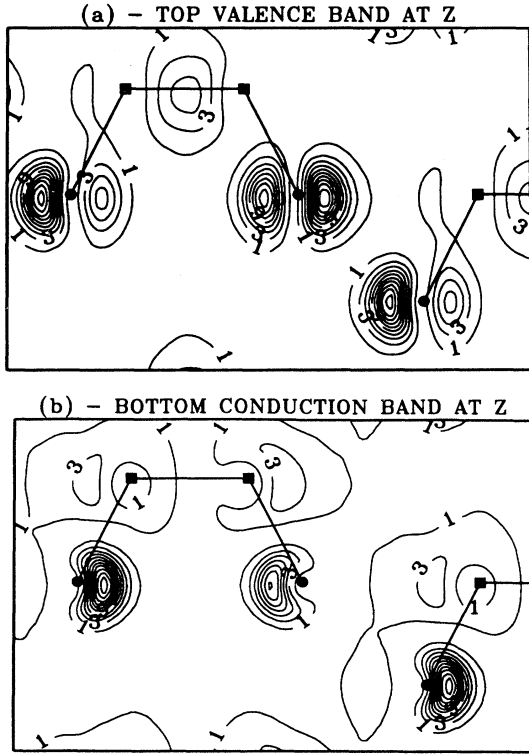


FIG. 7. Wave functions squared for γ -InSe; filled circles represent Se atoms and filled squares In atoms: (a) Wave function for the lowest conduction band at Z. (b) Wave function for the top valence band at Z.

determined from its electronic structure by fitting a parabola to $E(\mathbf{k}_0)$ at eight very close neighboring \mathbf{k} points and by finding the second derivative of this parabola. This was done for various different orthogonal directions, from which a reciprocal effective-mass tensor, conveniently interpreted on the basis of the $\mathbf{k}\cdot\mathbf{p}$ perturbation theory for a nondegenerate level E_n ,²² was built:

$$\frac{1}{m_{\alpha\beta}^*} = \pm \frac{1}{\hbar^2} \left[\frac{\partial^2 E}{\partial k_\alpha \partial k_\beta} \right]_{\mathbf{k}_0} = \pm \left[\frac{\delta_{\alpha\beta}}{m_0} + \frac{1}{m_0^2} \sum_{j \neq n} \frac{p_{nj}^\alpha p_{jn}^\beta + p_{nj}^\beta p_{jn}^\alpha}{E_n(\mathbf{k}_0) - E_j(\mathbf{k}_0)} \right]; \quad (1)$$

the positive and negative signs refer to the conduction and valence bands, respectively, \hbar denotes Planck's constant, m_0 the free-electron mass, k_α and k_β the Cartesian components of vector \mathbf{k} , and p_{nj}^α and p_{jn}^β the Cartesian components of the momentum matrix elements between the states n and j . By diagonalizing this tensor we calculated the effective masses along its principal axes; two axes are in the plane of the layers and the third axis is along the z axis. Table I gives the electron and hole effective masses parallel to the layers and in a direction normal to the plane of the layers at $\mathbf{k}_0 = Z$, the gap minimum for γ -InSe. Due to the absence of bonding between layers (as seen in Fig. 6), it might be expected that the masses in a direction perpendicular to the layers would be extremely large. However, Table I shows otherwise: the masses parallel to the layers are larger than the ones normal to the masses. This anomalous anisotropy in the masses has been studied previously for GaSe, a similar layered compound.^{3,23} Schlüter³ introduced an artificial potential barrier in his empirical pseudopotential calculations to reduce the interlayer interaction and so increase the anisotropy of the masses. This anomalous behavior is a consequence of the fact that the layers themselves have an internal structure. Figure 7(b) shows clearly a strong In-In bonding within a layer along the z axis. Figure 7(a) shows some antibonding between adjacent In atoms. These strong intralayer interactions lead to light out-of-plane masses for both the electrons and holes of $m_\perp = 0.03m_0$. The lateral in-plane interactions are smaller for the states at the valence maximum and conduction minimum at Z: Figure 7(b) shows the valence maximum state to be mainly Se p_z lone-pair nonbonding orbitals, with partial In-In σ_z bonding. The angular-momentum decomposition shows that the wave function corresponding to the top valence band is composed essentially of Se p_z orbitals (70%) and In p_z orbitals (30%): [in the case of the bottom conduction band, the

TABLE I. Electron and hole masses (in units of the free-electron mass) at the gap minimum for γ -InSe; m_{\parallel} means parallel to the layers and m_{\perp} means perpendicular to the layers.

$\mathbf{k} = Z$	Electron	Hole	Reduced
m_{\parallel}	0.12	3.1	0.12
m_{\perp}	0.03	0.03	0.015
\perp/\parallel	0.25	0.01	

angular-momentum decomposition shows the wave function to be composed of Se s orbitals (37.5%), Se p_z orbitals (25%), and In s orbitals (37.5%). The lack of lateral (xy) bonding in the top valence state leads to a large in-plane hole mass $m_{\parallel} = 3.1m_0$. The ratio m_{\perp}/m_{\parallel} is 0.25 for electrons and 0.01 for holes. The $m_{\perp}/m_{\parallel} < 1$ character is thus not “anomalous” at all: such behavior should only be expected in *monolayer* planar structures, not planar structures like InSe where the layers are composed of four-atomic-plane units. The calculated masses are expected to be smaller than the real masses; this is a consequence of the fact that the density-functional theory underestimates the energy gap in semiconducting phases and, from $\mathbf{k}\cdot\mathbf{p}$ theory [Eq. (1)], the masses as well.²⁴ The experimental value for the direct exciton reduced mass is $0.12m_0$ (Ref. 5) and we obtain $0.06m_0$, a factor of 2 smaller, consistent with the fact that LDA strongly underestimates the value of the gap. This should not, however, affect the above description of the gross features of m_{\perp} and m_{\parallel} .

IV. OPTICAL PROPERTIES

In order to calculate the optical properties of the crystal, we considered its density of states, as well as its joint density of states and complex dielectric function $\epsilon_2(\omega)$. Figure 8 shows the density of states of γ -InSe, defined as the number of states per unit energy inside a unit cell:

$$\text{DOS}(\epsilon) = \sum_n \int_{\text{BZ}} \frac{d^3k}{\Omega_{\text{BZ}}} \delta(\epsilon - \epsilon_{nk}), \quad (2)$$

where Ω_{BZ} is the volume of the first Brillouin zone and ϵ_{nk} are the one-electron energies. Our sampling of the \mathbf{k} points in the Brillouin zone is similar to a procedure by Lehmann and Taut,²⁵ where the Brillouin zone is divided into small tetrahedra, in which the integrand of the DOS integral is interpolated linearly, making possible the calculation of the integrals analytically. In these calculations the irreducible segment of the Brillouin zone was

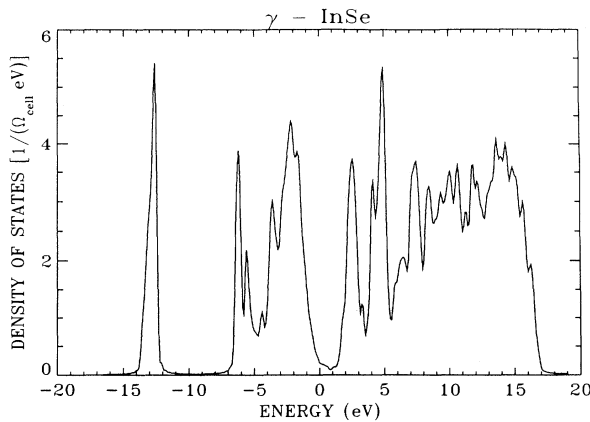


FIG. 8. Density of states for γ -InSe. The maximum of the valence band is at $E=0$. The fact that the density of states is not zero in the gap is due to the Gaussian broadening of $\sigma=0.2$ eV with which the original data were convoluted.

filled with 128 small tetrahedra. To account phenomenologically for the experimental line resolution, our results were convoluted with a Gaussian of width 0.2 eV. The calculations were done for the γ polytype only, since they are less computer time consuming and since the difference between the γ and β phases is small. As was said before, LDA calculations underestimate the energy gap; to correct this underestimate we have introduced a rigid shift of the conduction band that brings the optical

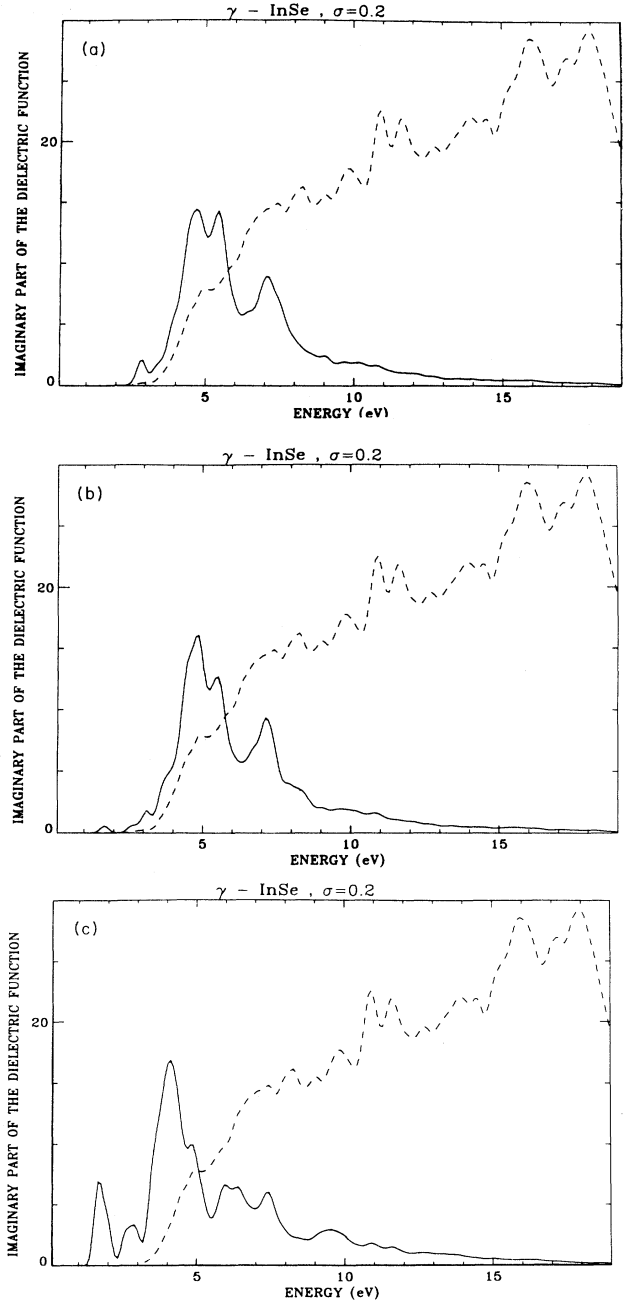


FIG. 9. Imaginary part of the dielectric function (solid line) and joint density of states (dashed line) for γ -InSe. (a) Polarization along x . (b) Polarization along y . (c) Polarization along z .

gap to 1.35 eV, the experimental value.²⁰ Apart from this energy gap, there can also be observed a gap between $\simeq -7.0$ and -12.5 eV separating the deep Se 4s orbitals from the other Se 4p and In 5s, 5p orbitals.⁷

A detailed numerical calculation of the joint density of states J_{cv} or the complex dielectric function ϵ requires the knowledge of $\epsilon(\mathbf{k})$ over the whole Brillouin zone. The joint density of states is

$$J_{cv}(\epsilon) = 2 \sum_{cv} \int_{\text{BZ}} \frac{d^3k}{\Omega_{\text{BZ}}} \delta[\epsilon - \Delta\epsilon_{cv}(\mathbf{k})], \quad (3)$$

where $\Delta\epsilon_{cv}(\mathbf{k})$ is the vertical transition energy between a conduction and a valence state (i.e., at same \mathbf{k}), and the imaginary part of the dielectric function is (neglecting excitonic effects)

$$\epsilon_2^\mu(\omega) = \frac{8\pi^2 e^2}{\hbar m_0^2 \omega^2} \sum_{cv} \int_{\text{BZ}} \frac{d^3k}{(2\pi)^3} |P_{cv}^\mu(\mathbf{k})|^2 \delta[\omega_{cv}(\mathbf{k}) - \omega], \quad (4)$$

where e is the electron charge, $P_{cv}^\mu = \langle v | \mathbf{e}_\mu \cdot \mathbf{p} | c \rangle$, and \mathbf{e}_μ is the unit vector in the direction μ . The imaginary part of the dielectric function and the joint density of states for the x , y , and z directions are plotted in Figs. 9(a), 9(b), and 9(c), respectively. The energy range goes from 0 eV at the top of the valence band to 19 eV. For light polarization parallel to the x direction, $\epsilon_2(\omega)$ starts far above the band gap at 2.5 eV, in excellent agreement with the experimental results of Kuroda, Munakata, and Nishina,²⁶ for the absorption coefficient when light is polarized parallel to the layers; the main peaks are around 4.8, 5.6, and 7.2 eV. These peaks are also salient in the y direction, but we see a small contribution at the gap edge. From our calculation of the oscillator strength, the peak at 2.5 eV arises from the transition from the flatband just below the gap (see Fig. 4) to the first conduction band. We obtained this result without any fitting, apart from the already explained “scissors operator” to adjust the LDA gap to the true experimental gap. The second flatband below the gap has no oscillator strength; the second peak in the absorption coefficient of Kuroda, Munakata, and Nishina,²⁶ at 2.9 eV comes from the degenerate first flatband below the gap when spin-orbit effects are included in the calculations; Fig. 5 shows a splitting of 0.3 eV, and both of the split flatbands have a strong oscillator strength value. We calculated $|P_{cv}^\parallel|^2/2m$ to be 3.0 eV, whereas the value established by Kuroda, Munakata, and Nishina is 3.9 eV; this difference might be due to their fitting of a theoretical curve to their experimental results. When the polarization is in the z direction, $\epsilon_2(\omega)$ is much richer in structures; the main peaks are around 1.8, 2.9, 4.2, 4.9, 6.1, 6.5, 7.5, and 9.5 eV. The existence of structure in $\epsilon_2^z(\omega)$ at the band edge, and its near absence in $\epsilon_2^x(\omega)$ and $\epsilon_2^y(\omega)$, can be understood from Fig. 6, where the wave functions at the edge of the gap are plotted; for both the valence and the conduction bands they have a distinctly z -axis character. In the dielectric function ex-

pression [Eq. (3)] there is a partial derivative operator inside the matrix element involving a valence state and a conduction state. If the wave functions consist of p_z orbitals of Se and In atoms, the matrix element will become zero when the partial derivative is $\partial/\partial x$ or $\partial/\partial y$. As we stated previously in Sec. III, the angular-momentum decomposition of the top valence band consists entirely of p_z orbitals of both In and Se. The oscillator strengths between the top valence and bottom conduction bands were also calculated and were found to be zero between these two bands for light polarization in the x and y directions. The calculated value for $|P_{cv}^\parallel|^2/2m$ is 2.11 eV. There is a large matrix element of $\partial/\partial z$ with respect to the bottom conduction state and the top valence state. In summary, the strong P_{cv}^\parallel oscillator strength is the origin of the difference at the band edge between $\epsilon_2^z(\omega)$ and $\epsilon_2^x(\omega)$, $\epsilon_2^y(\omega)$ or J_{cv} . The fact that at higher energies ϵ_2 decreases as opposed to the J_{cv} 's is due to the ω^2 factor in the denominator of Eq. (3).

V. CONCLUSION

We believe this to be the first *ab initio* local-density functional calculation of the electronic structure of γ -InSe and β -InSe. It can be said that these two layered compounds are essentially the same with respect to their electronic properties; given that the interlayer interactions are of the weak Van der Waals type, the relative arrangement of the layers does not affect the electronic structure very much. Relativistic effects were included for γ -InSe by accounting for the spin-orbit interaction; the effects are more important close to the band gap at the center of the Brillouin zone Γ , a splitting of the two top valence bands being the most salient feature. However, at the minimum of the gap at Z , there are no effects, the splitting of the bands occurring below the top valence band. Because of the uniaxial anisotropy of InSe, different effective masses parallel and perpendicular to the z axis are expected. However, due to the strong intraplanar interactions within a single four-atomic-plane layer, the out-of-plane masses for both electrons and holes are lighter than their in-plane counterparts. This explains the “anomalous” behavior cited earlier.^{3,23} Optical properties were discussed in Sec. IV by the study of the density of states, joint density of states, and the imaginary part of the dielectric function. Optical properties for γ -InSe were studied by calculating the density of states, the joint density of states, and the imaginary part of the dielectric function. The xy versus z anisotropy in the dielectric function is evident in the very low intensity of $\epsilon_2(\omega)$ close to the gap when the polarization is along the x or y directions, as opposed to the high intensity just above the gap for a polarization along the z axis. As discussed in the preceding section, this is due to the p_z character of the two wave functions delimiting the gap.

- ¹P. Gomes da Costa, M. Balkanski, and R. F. Wallis, *Phys. Rev. B* **43**, 7066 (1991).
- ²P. Gomes da Costa, M. Balkanski, and R. F. Wallis, in *Festschrift for Professor Rogério Leite*, edited by M. Balkanski, C. E. T. Gonçalves da Silva, and J. M. Worlock (World Scientific, Singapore, 1991), p. 83.
- ³M. Schlüter, *Nuovo Cimento B* **13**, 313 (1973).
- ⁴J. V. McCanny and R. B. Murray, *J. Phys. C* **10**, 1211 (1977).
- ⁵A. Bourdon, A. Chevy, and J. M. Besson, in *Physics of Semiconductors 1978*, Proceedings of the 14th International Conference on the Physics of Semiconductors, edited by B. L. H. Wilson, IOP Conf. Proc. No. 43 (Institute of Physics and Physical Society, London, 1979), p. 1371.
- ⁶J. Robertson, *J. Phys. C* **12**, 4777 (1979).
- ⁷E. Doni, R. Girlanda, V. Grasso, A. Balzarotti, and M. Piacentini, *Nuovo Cimento B* **51**, 154 (1979).
- ⁸M. Piacentini, E. Doni, R. Girlanda, V. Grasso, and A. Balzarotti, *Nuovo Cimento B* **54**, 269 (1979).
- ⁹Y. Depeursinge, *Nuovo Cimento B* **64**, 111 (1981).
- ¹⁰K. Kunc and R. Zeyher, *Europhys. Lett.* **7**, 611 (1965).
- ¹¹P. Hohenberg and W. Kohn *et al.*, *Phys. Rev.* **136**, B284 (1964); W. Kohn and L. J. Sham, *ibid.* **140**, A1133 (1965).
- ¹²J. Ihm, A. Zunger, and M. L. Cohen, *J. Phys. C* **12**, 4409 (1979).
- ¹³G. Kerker, *J. Phys. C* **13**, L189 (1980).
- ¹⁴D. M. Ceperley and B. J. Alder, *Phys. Rev. Lett.* **45**, 566 (1980).
- ¹⁵D. J. Chadi and M. L. Cohen, *Phys. Rev. B* **8**, 5757 (1973); H. J. Monkhorst and J. D. Pack, *ibid.* **13**, 5188 (1976).
- ¹⁶J. E. Dennis, Jr. and J. J. Moré, *SIAM Rev.* **19**, 46 (1977); P. Bendt and A. Zunger, *Phys. Rev. B* **26**, 3114 (1982).
- ¹⁷J. P. Perdew and A. Zunger, *Phys. Rev. B* **23**, 5048 (1981).
- ¹⁸M. S. Hybertson and S. G. Louie, *Phys. Rev. B* **34**, 2920 (1986).
- ¹⁹J. C. Slater, *Quantum Theory of Molecules and Solids* (McGraw-Hill, New York, 1965), Vol. 2.
- ²⁰M. Balkanski, C. Julien, and M. Jouanne, *J. Power Sources* **20**, 213 (1987).
- ²¹R. le Toullec, M. Balkanski, J. M. Besson, and A. Kuhn, *Phys. Lett.* **55A**, 245 (1975).
- ²²E. O. Kane, *J. Phys. Chem. Solids* **1**, 82 (1955); **1**, 249 (1957).
- ²³G. Ottaviani, C. Canali, F. Nava, P. Schmid, E. Moser, R. Minder, and I. Zschokke, *Solid State Commun.* **14**, 933 (1974).
- ²⁴X. Zhu, M. S. Hybertsen, and S. G. Louie, in *Atom Scale Calculations of Structure in Materials*, edited by M. S. Daw and M. A. Schlüter, MRS Symposia Proceedings No. 193 (Materials Research Society, Pittsburgh, 1990), p. 113.
- ²⁵G. Lehmann and M. Taut, *Phys. Status Solidi B* **54**, 469 (1972).
- ²⁶N. Kuroda, I. Munakata, and Y. Nishina, *Solid State Commun.* **33**, 687 (1980).